Chapter 13

Optimal Design of Refinery Hydrogen System With Purification Unit

Chun Deng* **and Xiao Feng†**

[*]State Key Laboratory of Heavy Oil Processing, College of Chemical Engineering, China University of Petroleum, Beijing, China, [†]School of Chemical Engineering & Technology, Xi'an Jiaotong University, Xi'an, China

13.1 INTRODUCTION

The amount of inferior crude oil being processed has been increasing yearly all over the world. For example, Sinopec, one of the main Chinese refinery companies, imported up to 70 million tons of high-sulfur crude oil in 2010 and the annual growth rate is around 17%. The environmental regulations and policies on sulfide contained in product oil have become tighter recently. Both the European Standard (EN 228+A1-2017) and Chinese standard (GB 17930-2016) specify unleaded petrol with a maximum sulfur content of 0.001%. Refineries have been increasing the processing ratio of hydrotreating and hydrocracking processes, which consume a large amount of hydrogen. The hydrogen deficit aggravates the fresh hydrogen shortage in refineries, making fresh hydrogen a more and more expensive resource for modern refineries. Hydrogen production technologies, such as steam reforming of natural gas or methane, are commonly utilized to produce hydrogen to supplement the deficit. However, hydrogen production is a typical high energy consumption process. Synthesis of refinery hydrogen network has been an effective tool to recover hydrogen and reduce the capacity of the hydrogen plant. The methodologies on synthesis of a refinery hydrogen network can be categorized into two types: insight-based pinch technique and the superstructure-based mathematical programming approach.

This chapter is organized as follows. In the following section, we provide a brief introduction of the hydrogen system of a refinery plant. After that, the pinch technique is presented for the targeting of a hydrogen network

Hydrogen Supply Chain. https://doi.org/10.1016/B978-0-12-811197-0.00013-0

with purification reuse/recycle. Then, the superstructure-based mathematical programming approach for the optimal design of a hydrogen network is introduced before the conclusion of the chapter.

13.2 HYDROGEN SYSTEM OF REFINERY PLANT

In this section, an overview of a refinery hydrogen system and its elements is briefly introduced. This is followed by the introduction of a process flow schematic diagram for typical consumers (i.e., hydrocracking) and hydrogen producers (i.e., hydrogen plant). The purification processes, including cryogenic separation, pressure swing adsorption, membrane, light hydrocarbon recovery, and desulfurization, are summarized at the end of this section. An overall view of a refinery hydrogen system is illustrated in Fig. 13.1 and it includes the hydrogen consumers (i.e., hydrocracking, hydrotreating units) and hydrogen sources (i.e., catalytic reforming, hydrogen plant), as well as the purification units (i.e., H_2S removal and PSA).

13.2.1 Typical Hydrogen Consumers

In a modern refinery the demand for petroleum products has shifted from diesel fuel and heating oil to high ratios of gasoline and jet fuel. Environmental regulations limiting sulfur and aromatic contents in motor fuels are stricter.

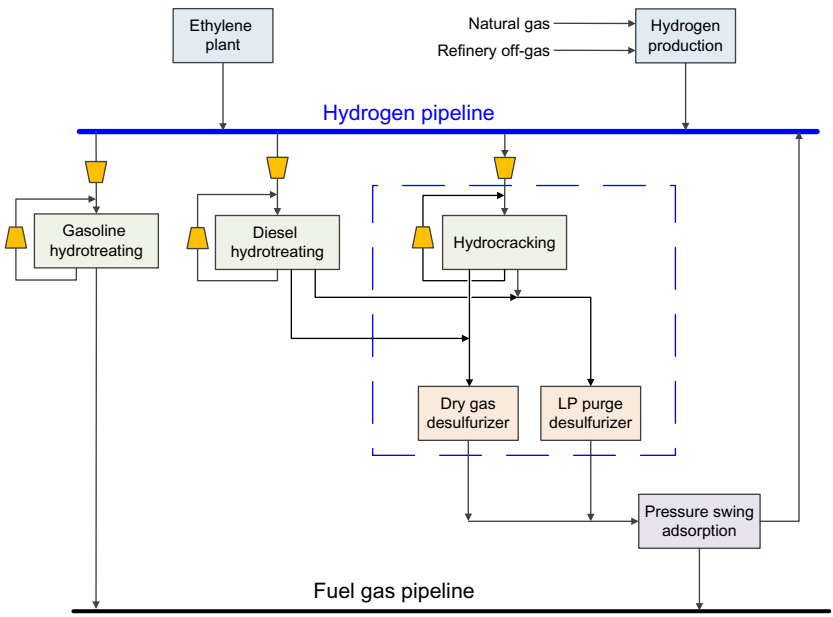

FIG. 13.1 Overall schematic view of a refinery hydrogen network.

These factors lead to the widespread use of hydrocracking in a modern refinery. Catalytic cracking superimposed with hydrogenation is the mechanism of hydrocracking. Catalytic cracking is the breaking of a carbon–carbon single bond, and hydrogenation is the addition of hydrogen to a carbon–carbon double bond. Typical hydrocracker feedstocks include kerosene, straight-run diesel, atmospheric gas oil, vacuum gas oil, fluid catalytic cracking (FCC), light cycle oil (FCC LCO) and heavy cycle oil (HCO), Light Coker Gas Oil (LCGO), and Heavy Coker Gas Oil (HCGO). The aromatic cycle oils and coker distillates are very refractory and resist catalytic cracking. The higher pressures and hydrogen atmosphere make them relatively easy to hydrocrack. The products of hydrocracker mainly include naphtha, and/or jet fuel, diesel, and lube oil (Gary and Handwerk, 2001).

Hydrotreating processes are to catalytically stabilize petroleum products and/or remove objectionable elements from products or feedstocks by the reaction in the presence of hydrogen. Stabilization usually indicates that the unsaturated hydrocarbons, such as olefins and unstable diolefins, are converted to paraffin. Objectionable elements, including sulfur, nitrogen, oxygen, halides, and trace metals, are removed by hydrotreating. The process can be applied to a wide range of feedstocks, from naphtha to reduced crude. Once the process is employed specifically for sulfur removal, it is usually called hydrodesulfurization, or HDS. In order to fulfill environmental regulations, hydrogenation may be conducted on aromatic rings to decrease aromatic content by converting aromatics to paraffin via the hydrotreating process (Gary and Handwerk, 2001).

A simplified process diagram for the hydrocracking process is illustrated in Fig. 13.2. Note that it is similar to the process diagram for hydrotreating. The fresh liquid feed is mixed with makeup hydrogen and recycle gas stream, which is rich in hydrogen content and passed through a heat exchanger to recover the heat of the effluent of the reactors. A furnace is applied to heat the mixed feed to the required temperature. If the liquid feed has not been hydrotreated, a guard reactor should be placed before the first hydrocracker. The guard reactor is

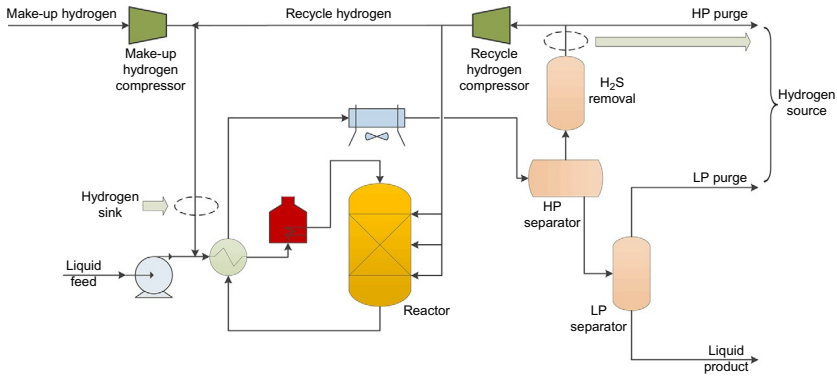

FIG. 13.2 Typical schematic process diagram for hydrocracking process.

usually used to convert organic sulfur and nitrogen compounds to hydrogen sulfide, ammonia, and hydrocarbons to protect the precious metal catalyst found in the following reactors. The hydrocracking reactor(s) is operated at a sufficiently high temperature to convert 40–50 vol% of the reactor effluent to material boiling below 205°C. The reactor effluent goes through heat exchangers (may include air cooler) to a high-pressure separator where the hydrogen-rich gases are separated. The gas stream separated from the high-pressure separator may pass through an absorber to remove H_2S prior to being recycled to the first stage for mixing both makeup hydrogen and fresh feed, or it may be fed to intervals of catalyst bed as coolant for temperature control. Portion of the sweetened gas may be purged to the fuel system to avoid the buildup of unfavorable components. The liquid product from the high-pressure separator is sent to a low-pressure separator where the hydrogen gas (so-called low-pressure purge) is separated and then discharged to the fuel system. The liquid effluent from the low-pressure separator is allocated to a distillation column where the C4 and lighter gases are separated overhead, and the light and heavy naphtha, jet fuel, and diesel fuel boiling range streams are removed as liquid side-products. The fractionator bottoms can be partially or totally recycled as the feed of the hydrocracking (Gary and Handwerk, 2001).

Note that, the sweetening high-pressure/low-pressure separator gas streams can be considered as process hydrogen sources. The inlets of the hydrogenation reactors act as process hydrogen sinks, which require hydrogen streams with specified flowrate and pressure as well as hydrogen content.

For the kth hydrogen sink, the inlet flowrate and hydrogen purity can be calculated via Eqs. (13.1), (13.2).

$$F_k^{\text{in}} = F_k^{\text{M}} + F_k^{\text{R}} \tag{13.1}$$

$$y_{k,\text{H}_2}^{\text{in}} = \frac{F_k^{\text{M}} y_{\text{H}_2}^{\text{M}} + F_k^{\text{R}} y_{\text{H}_2}^{\text{R}}}{F_k^{\text{in}}} \tag{13.2}$$

where F_k^{in}, F_k^{M} and F_k^{R} denote the flowrate of total inlet, make-up and recycle hydrogen streams for the kth hydrogen sink, mol s^{-1}. $y_{k,\text{H}_2}{}^{\text{in}}$, $y_{\text{H}_2}{}^{\text{M}}$ and $y_{\text{H}_2}{}^{\text{R}}$ represent the hydrogen mole fractions of inlet for the kth hydrogen sink, make-up and recycle hydrogen streams. In addition, the make-up hydrogen and recycle hydrogen compressors are placed to lift the pressure of hydrogen sources to fulfill the pressure requirement of hydrogen sinks.

13.2.2 Typical Hydrogen Producers

The increasing demand of high-octane gasoline has stimulated the use of catalytic reforming. With the implementation of restrictions on the aromatic contents of gasoline, catalytic reforming is expected to decrease. However, the increasing demand for the derivative product of p-Xylene (PX), as its core

source, the processing ratio of catalytic reforming keeps increasing. In the catalytic reforming process, the hydrocarbon molecular structures are rearranged to form higher-octane aromatics and a small amount of cracking would occur. The process aims to increase the octane number of gasoline. The hydrogen-rich gas stream from the catalytic reforming process is split into a hydrogen recycle stream and a net hydrogen byproduct that acts as the main hydrogen source for hydrocracking or hydrotreating processes (Gary and Handwerk, 2001).

Additional hydrogen for extensive hydrocracking and hydrotreating processes can be provided via partial oxidation of heavy hydrocarbons (i.e., fuel oil), or stream reforming of methane (natural gas), ethane, or propane. Compared with partial oxidation of fuel oil, the cost for hydrogen production via steam reforming of methane is usually lower and it is more widely used in industry (Gary and Handwerk, 2001). In addition, the syngas from coal gasification serves as another hydrogen source.

Steam-methane reforming (SMR) for hydrogen production includes four steps: reforming, shift conversion, gas purification, and methanation. A simplified flow diagram is presented in Fig. 13.3. Firstly, the catalytic reaction of methane with steam at temperatures in the range of 760–816°C is endothermic and is carried out by passing the gas through catalyst-filled tubes in a furnace. In the second step, more steam is added to convert the CO generated in the first step to an equivalent amount of hydrogen via the shift reaction. It is an exothermic reaction and is carried out in a fixed-bed catalytic reactor at around 343°C. There are multiple catalyst beds in one reactor and external cooling exists between beds to prevent the temperature from getting too high, as that would adversely affect the equilibrium conversion. The generated CO_2 is removed in the third step by adsorption in a circulation amine or hot potassium carbonate solution and the rich solution is regenerated in a stripper. In the fourth step, the remaining small amount of CO and CO_2 are converted to methane via methanation reactions, which are exothermic. This is conducted in a fixed-bed reactor at a temperature of 427°C (Gary and Handwerk, 2001). Note that the gas purification and methanation can be replaced via pressure swing adsorption (PSA). The carbon dioxide and other impurities can be removed via PSA and the purity of the product stream of PSA can reach 99% or even higher.

13.2.3 Industrial Hydrogen Purification Process

A significant amount of the hydrogen-rich gas stream is vented from hydrocracking or hydrotreating processes. Recovery of the hydrogen should be taken

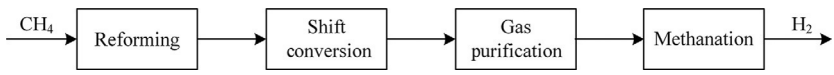

FIG. 13.3 Block diagram of steam-methane reforming process for hydrogen production.

into consideration whenever it is needed to supplement the hydrogen demand. Typical processes for hydrogen recovery include cryogenic phase separation, pressure swing adsorption, and membrane.

In the cryogenic phase separation method, the feed gas stream is cooled to around −129 to −157°C at pressures ranging from 1380 to 3450 kPa. The resulting vapor phase contains 90 mol% hydrogen and the liquid phase includes most of methane and other hydrocarbons. The carbon dioxide, hydrogen sulfide, and water vapor must be removed from the feed gas prior to chilling (Gary and Handwerk, 2001).

In the pressure swing adsorption process, hydrocarbon is absorbed from the gas on a solid absorbent (i.e., molecular sieve) and hydrogen leaves the absorber at the desired purity. Several adsorbent columns are used, and the feed gas flow is periodically switched from one column to another so that the adsorbent can be regenerated. The adsorbed methane and other impurities are released from the adsorbent by simple pressure decline and purging (Gary and Handwerk, 2001).

In the membrane process, a membrane composed of synthetic hollow fibers, which allow hydrogen to permeate, separates hydrogen from methane and other components. The driving force is the difference between the hydrogen partial pressures on each side of the membrane. Thus a significant pressure drop must be imposed in order to achieve high recovery (Gary and Handwerk, 2001).

The most economical technique for hydrogen recovery depends on the volume of the gas stream to be processed, the desired hydrogen recovery and purity, and the types of components to be separated (Gary and Handwerk, 2001).

The valuable C_3, C_4, C_5, and C_6 components contained in the gas streams can be recovered via the gas processing units, so-called light hydrocarbon recovery. Typical light hydrocarbon recovery processes include absorber-deethanizer, sponge absorber, depropanizer, debutanizer, and naphtha splitter. A brief introduction to the process can be found in the literature (Gary and Handwerk, 2001).

In addition, gas streams from various processes in the refinery processing of sour crudes contain hydrogen sulfide. Some dissolved carbon dioxide may be contained in the gas streams. Those components (hydrogen sulfide and carbon dioxide) are typically called acid gases. They can be removed by many processes, which can be categorized into three kinds: chemical solvent (i.e., monoethanolamine (MEA), diethanolamine (DEA), methyl-diethanolamine (MDEA), diglycolamine (DGA), hot potassium carbonate), physical solvent (i.e., selexol, propylene carbonate, sulfinol, rectisol), and dry adsorbents processes (i.e., molecular sieve, activated charcoal, iron sponge, zinc oxide). Generally, the diethanolamine process has been the most widely used for treating refinery gas. This process uses an aqueous solution of diethanolamine with concentrations of the DEA in the range of 15–30 wt% (Gary and Handwerk, 2001).

13.3 TARGETING HYDROGEN NETWORK VIA PINCH TECHNIQUE

The Pinch technique has been accepted as an effective tool for the targeting and design of a hydrogen network. Typically, the Pinch technique includes two steps: targeting and design. Alves and Towler (2002) first introduced the Hydrogen Surplus Diagram to identify the pinch and locate the minimum flowrate of hydrogen utility prior to detailed network design. Many other insight-based pinch techniques, such as Material Recovery Pinch Diagram (El-Halwagi et al., 2003), Source Composite Curve (Bandyopadhyay, 2006), Gas Cascade Analysis (Foo and Manan, 2006), Material Surplus Composite Curve (Saw et al., 2011), Composite Algorithm Table (Agrawal and Shenoy, 2006), and extended Limiting Composite Curve (Agrawal and Shenoy, 2006), have been developed to determine the flowrate targets for hydrogen networks. On the basis of the extension of the Composite Algorithm Table, we presented the Improved Problem Table (IPT) (Deng et al., 2015) to target the hydrogen network with purification units.

13.3.1 Model for Hydrogen Network With One Purifier

Prior to the flowrate targeting procedure, the mass balance for a hydrogen network with purification reuse/recycle is addressed (Deng et al., 2015). Fig. 13.4 illustrates the mass flows for a hydrogen network with purification reuse/recycle. The mass balance around the purifier is given by Eqs. (13.3), (13.4). In addition, the hydrogen recovery ratio (*RR*) is defined by Eq. (13.5).

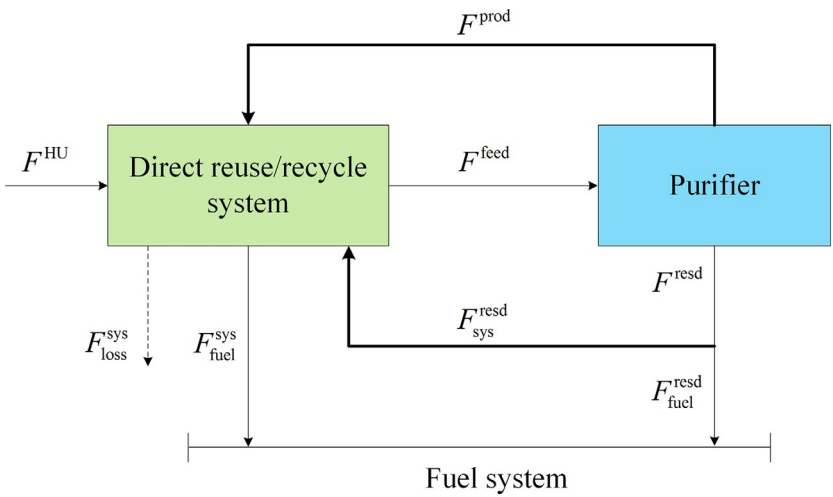

FIG. 13.4 Schematic diagram for mass flows of the hydrogen network with purification reuse/recycle (Deng et al., 2015).

$$F^{\text{feed}} = F^{\text{prod}} + F^{\text{resd}} \tag{13.3}$$

$$F^{\text{feed}} y_{H_2}^{\text{feed}} = F^{\text{prod}} y_{H_2}^{\text{prod}} + F^{\text{resd}} y_{H_2}^{\text{resd}} \tag{13.4}$$

$$RR = \frac{F^{\text{prod}} y_{H_2}^{\text{prod}}}{F^{\text{feed}} y_{H_2}^{\text{feed}}} \tag{13.5}$$

where F^{feed}, F^{prod}, and F^{resd} denote the feed, product, and residual flowrate of the purifier and their hydrogen purities are specified as $y_{H_2}^{\text{feed}}$, $y_{H_2}^{\text{prod}}$ and $y_{H_2}^{\text{resd}}$. The optimal F^{prod} can be determined via IPT (introduced in Step 6) with the specified $y_{H_2}^{\text{prod}}$. There are two options for the residual flowrate of the purifier: reuse/recycled by hydrogen sinks in the direct reuse/recycle system ($F_{\text{sys}}^{\text{resd}}$) or discharged to the fuel system ($F_{\text{fuel}}^{\text{resd}}$) and the flowrate balance is given by Eq. (13.6).

$$F^{\text{resd}} = F_{\text{sys}}^{\text{resd}} + F_{\text{fuel}}^{\text{resd}} \tag{13.6}$$

The overall mass balance is given by Eq. (13.7).

$$F^{\text{HU}} = F_{\text{loss}}^{\text{sys}} + F_{\text{fuel}}^{\text{sys}} + F_{\text{fuel}}^{\text{resd}} \tag{13.7}$$

where $F_{\text{fuel}}^{\text{sys}}$ and $F_{\text{fuel}}^{\text{resd}}$ denote the flowrates that discharged from the direct reuse/recycle system and residual of the purifier to the fuel system. $F_{\text{loss}}^{\text{sys}}$ denotes the total flowrate loss for the direct reuse/recycle system and it can be determined via Eq. (13.8). It is identical with the net flowrate in the last impurity interval determined in Step 2 of IPT. Note that, $F_{\text{loss}}^{\text{sys}}$ keeps unchanged if the system is selected. To minimize the flowrate of the hydrogen utility, $F_{\text{fuel}}^{\text{sys}}$ and $F_{\text{fuel}}^{\text{resd}}$ should be minimized as well.

$$F_{\text{loss}}^{\text{sys}} = \sum_{k}^{NSK} F_{SKk} - \sum_{i}^{NSR} F_{SRi} \tag{13.8}$$

The overall mass balance around the direct reuse/recycle system is given by Eq. (13.9).

$$F^{\text{HU}} + F^{\text{prod}} + F_{\text{sys}}^{\text{resd}} = F_{\text{loss}}^{\text{sys}} + F_{\text{fuel}}^{\text{sys}} + F^{\text{feed}} \tag{13.9}$$

13.3.2 Improved Problem Table

Next, IPT (Deng et al., 2015) is used to locate the targets for a refinery hydrogen network with purification reuse/recycle scheme. The targets include the minimum flowrates of hydrogen utility, feed and product flowrate of the purifier, and the optimal feed purity of the purifier. The optimal placement of the purifier corresponds to the optimization of its feed purity/impurity. We use an example to show the IPT. The limiting data shown in Table 13.1 are extracted from the literature (Elkamel et al., 2011). The hydrogen purity for the product of

TABLE 13.1 Limiting Data of Case 1

Hydrogen Sources	Purity (Fraction)	Flowrate (Nm^3/h)	Hydrogen Sinks	Purity (Fraction)	Flowrate (Nm^3/h)
HC	0.8	60,678	HC	0.8671	93,306
CR	0.8	17,303	GOHT	0.8358	82,656
GOHT	0.75	55,281	RHT	0.8257	39,164
RHT	0.75	25,870	DHT	0.7230	12,472
DHT	0.65	8004	NHT	0.7148	5726
NHT	0.6	3840			
Hydrogen utility	0.95	89,304 (current)			

the purifier is given as 0.9 and hydrogen recovery is defined as 0.9. The maximum inlet flowrate for the purifier is assumed to be 35,712 Nm^3/h. Because the purity of the purification product is known, the product of the purifier can be treated as an external hydrogen source.

Step 1: Purities and impurities arrangement: All of the purities of process hydrogen sources and sinks, as well as hydrogen utility and product stream of purifier, are arranged in decreasing order in the first column (Table 13.2). One value for duplicate purities (if any) is kept listed in the column. The arbitrary purity is added as the last entry of the column such that it is the smallest value, i.e., 0.55 in the first column. The arbitrary purity serves to provide an endpoint and facilitates the plotting of the last segment of the LCC. The second column shows the impurities (y^{ν}), which are determined by $1-y_{H_2}{}^{\nu}$. The impurities in the second column fulfil the relationship shown as Eq. (13.10).

$$y^1 < y^2 < \cdots < y^{\nu} < \cdots < y^{arbitrary} \tag{13.10}$$

Step 2: Net flowrate deficits targeting: The net flowrates F^{ν}_{net} in the third column (Table 13.2) are calculated by subtracting the summation of the flowrates of the hydrogen sources from those of the hydrogen sinks in each impurity interval. Once the impurities of the hydrogen sources and sinks are less than y^{ν}, these hydrogen sources and sinks will appear in the impurity interval (y^{ν}, $y^{\nu-1}$), and the net flowrate of this impurity interval can be calculated by Eq. (13.11). For instance, within the impurity interval (0.2, 0.25), there exist two process hydrogen sources (HC (0.2) and CR (0.2)) and three process hydrogen sinks (HC (0.1329), GOHT (0.1642) and RHT (0.1743)) in the impurity interval. The net flowrate can be calculated as 137,146 Nm^3/h by solving Eq. (13.11).

$$F^{\nu}_{net} = \sum_k F^{SKk} - \sum_i F^{SRi} \quad \forall y^{SRi},\ y^{SKk} < y^{\nu} \tag{13.11}$$

Note that the last entry of the third column of Table 13.2 is obtained by subtracting the summation of all flowrates of process hydrogen sources from that of process hydrogen sinks and it can be defined as the total flowrate deficit for a network. For a given hydrogen network, the total flowrate deficit is a constant and it indicates that at least such a flowrate of external hydrogen sources shall be supplemented for the network. For this case, the minimum flowrate for external hydrogen sources is 62,349 Nm^3/h, as indicated by the last entry in the third column.

Step 3: Net mass loads targeting: The net mass loads in the fourth column (Table 13.2) are calculated using Eq. (13.12). The net mass load for each impurity interval is the product of the net flowrate and the impurity difference of the corresponding interval.

$$\Delta M^{\nu}_{net} = F^{\nu}_{net}\left(y^{\nu} - y^{\nu-1}\right) \tag{13.12}$$

TABLE 13.2 Implementation of IPT for Case 1 With Purification Reuse/Recycle (Preliminary Solution) (Deng et al., 2015)

Purity (Fraction)	Impurity (Fraction)	Net Flowrate (Nm^3/h)	Net Load (Nm^3/h)	Cumulative Load (Nm^3/h)	Hydrogen Utility (Nm^3/h)	Flowrate for Purification Product (Nm^3/h)	Flowrate Above Pinch (Nm^3/h)	Flowrate Above Pinch (Nm^3/h)	Flowrate Above Pinch (Nm^3/h)	Flowrate for Waste Hydrogen Stream (Nm^3/h)
0.95	0.05			0	0					
		0	0							
0.9	0.1			0	0					
		0	0							
0.8671	0.1329			0	0	0				
		93,306	2917							
0.8358	0.1642			2917	25,549	45,454				
		175,962	1783							
0.8257	0.1743			4700	37,808	63,247				
		215,127	5526							
0.8	0.2			10,226	68,175	102,262				
		137,146	6857							
0.75	0.25			17,084	85,418	113,890				45,082
		55,995	1512							

Continued

TABLE 13.2 Implementation of IPT for Case 1 With Purification Reuse/Recycle (Preliminary Solution) (Deng et al., 2015)—cont'd

Purity (Fraction)	Impurity (Fraction)	Net Flowrate (Nm^3/h)	Net Load (Nm^3/h)	Cumulative Load (Nm^3/h)	Hydrogen Utility (Nm^3/h)	Flowrate for Purification Product (Nm^3/h)	Flowrate Above Pinch (Nm^3/h)	Flowrate Above Pinch (Nm^3/h)	Flowrate Above Pinch (Nm^3/h)	Flowrate for Waste Hydrogen Stream (Nm^3/h)
0.7230	0.277			18,596	81,917	105,057	55,994			
		68,467	562							
0.7148	0.2852			19,158	81,448	103,436	58,901			
		74,193	4807							
0.65	0.35			23,964	79,881	95,858	68,808			2619
		66,189	3309							
0.6	0.4			27,274	77,925	90,913	67,935	66,189		3840
		62,349	3117							
0.55	0.45			30,391	75,978	86,832	66,538	64,269	62,349	

Eqs. (13.12), (13.11)	$F^{feed}y_{H_2}{}^{feed}$	$F^{prod}y_{H_2}{}^{prod}$	$F^{resd}y_{H_2}{}^{resd}$	$y_{H_2}{}^{feed}$	F^{feed}	$\sum F^{WH}$	$F^{feed}y_{H_2}{}^{feed}$
	113,890	*102,501*	*11,389*	**0.734**	*155,218*	51,542	*103,677*
Eq. (13.9)	F_{HU}	F^{prod}	F^{resd}_{sys}	F^{sys}_{loss}	F^{feed}	F^{sys}_{fuel}	$\sum F^{WH} - F^{feed}$
	0	**113,890**	**0**	**62,349**	**51,542**	**0**	0

Step 4: Cumulative mass loads targeting: The cumulative mass loads are calculated in the fifth column (Table 13.2) using Eq. (13.13). The first entry for the column has no cumulative mass load so that it equals zero. The cumulative mass load of the vth row is determined by the summation of the mass loads for all earlier rows.

$$\begin{aligned} \Delta M_{cum}^{v} &= 0 \qquad\qquad v = 1 \\ \Delta M_{cum}^{v} &= \sum_{t=1}^{t=v} \Delta M_{net}^{t} \quad v > 1 \end{aligned} \tag{13.13}$$

The LCC can be constructed via plotting the cumulative load column as abscissa against the impurity column as ordinate, as shown in the bold line in Fig. 13.5. The reciprocal of the slope of a segment on the LCC corresponds to the net flowrate of the same impurity interval determined in Step 2. Note that the reciprocal of the slope of the last segment of the LCC is identical with the total flowrate deficit of the network.

Step 5: Flowrate targeting for hydrogen utility: The possible supply flowrates for hydrogen utility at each impurity level (y^{v}) in the sixth column are calculated using Eq. (13.14).

$$F^{HU} = \frac{\Delta M_{cum}^{v}}{y^{v} - y^{HU}} \tag{13.14}$$

where ΔM_{cum}^{v} and y^{v} denotes the cumulative mass load and impurity for the vth impurity level and y^{HU} denotes the impurity of hydrogen utility.

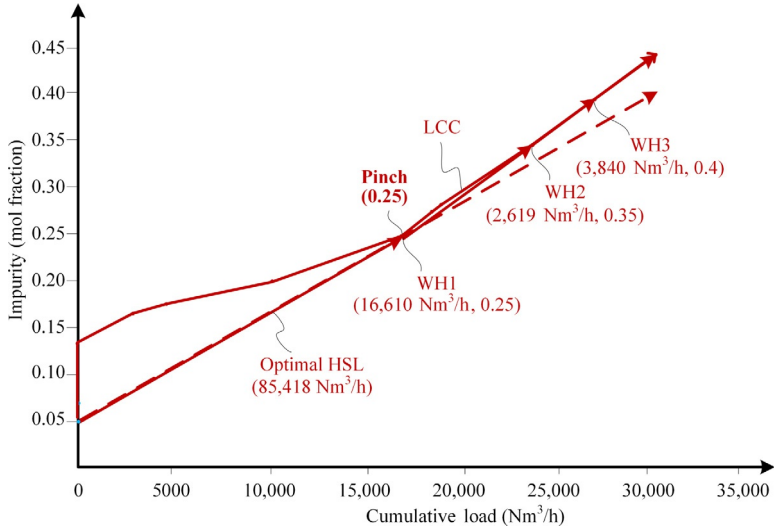

FIG. 13.5 LCC and optimal HSL with direct reuse/recycle (Deng et al., 2015).

The maximum value in the sixth column of Table 13.2 is 85,418 Nm^3/h and it is marked in bold. It is greater than the total flowrate deficit (62,349 Nm^3/h) determined in Step 2 and the maximum value (85,418 Nm^3/h) is the minimum flowrate of hydrogen utility. The corresponding impurity (0.25) is identified as the pinch impurity.

If the maximum value in the sixth column (calculated by solving Eq. 13.14) is smaller than the total flowrate deficit determined in Step 2, the total flowrate deficit is taken as the minimum flowrate of hydrogen utility for the network. In this case, the HSL that touches the LCC would be infeasible. The optimal and feasible HSL should be in parallel with the last segment of the LCC as shown in Fig. 13.6.

Step 6: Flowrate targeting for other external hydrogen sources: All possible flowrates of other external hydrogen sources are calculated in the following columns. Note that if several external hydrogen sources with different impurities are available, an external hydrogen source with higher impurity (typically with lower cost) should be introduced prior to one with lower impurity (typically with higher cost) to fulfill the requirement of the sinks so that refineries can cut down on cost.

The impurity corresponding to the maximum value of all possible flowrates for the first external hydrogen source (HU_1) determined in Step 5 defines its pinch impurity ($y_{HU_1}^{\text{pinch}}$). The introduction of a second external hydrogen source (HU_2) with impurity of y^{HU_2} ($y^{HU_1} < y^{HU_2}$), if and only if the condition ($y^{HU_2} < y_{HU_1}^{\text{pinch}}$) is fulfilled, can reduce the flowrate for the first external

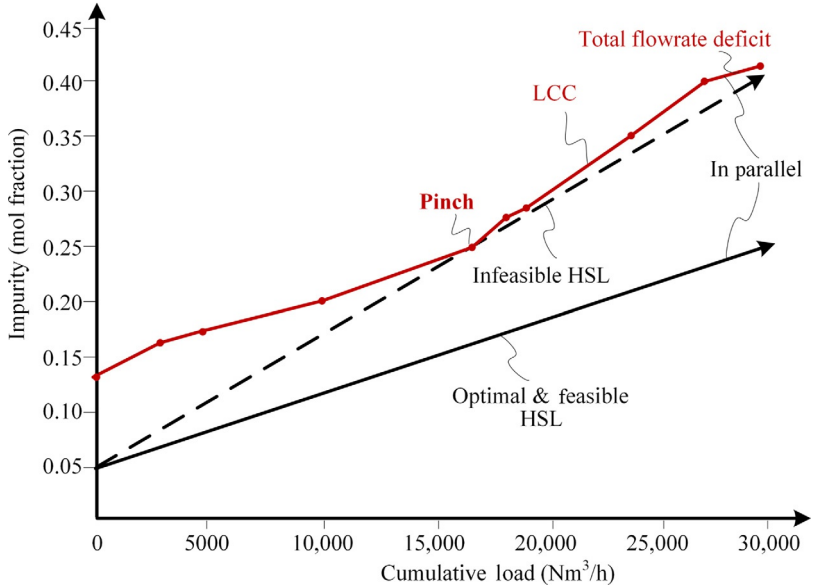

FIG. 13.6 Optimal and feasible HSL (Deng et al., 2015).

hydrogen source (F^{HU_1}) further. Typically, the value for the possible F^{HU_1} at the impurity level of y^{HU_2} is found as the optimal flowrate of the first external hydrogen source. Next, all the possible flowrates of the second external hydrogen source (HU_2) may be calculated using Eq. (13.15). This equation can be explained as follows. The first term of the numerator on the right-hand side (RHS) of Eq. (13.15) denotes the load between impurity interval [y^{HU_1}, y^{ν}]. The load removed by HU_1 is determined by the second term of the numerator on the RHS of Eq. (13.15). The first term on the RHS of Eq. (13.15) is solved to get the summation flowrate of HU_1 and HU_2. Next, the optimal flowrate of HU_1 is subtracted from the summation flowrate of HU_1 and HU_2 and the residual flowrate can be determined as the target of HU_2.

$$F^{HU_2} = \frac{\Delta M^{\nu}_{cum} - F^{HU_1}\left(y^{HU_2} - y^{HU_1}\right)}{y^{\nu} - y^{HU_2}} - F^{HU_1} \tag{13.15}$$

In order to calculate all the possible flowrates for the rth external hydrogen sources, Eq. (13.15) can be generalized to Eq. (13.16).

$$F^{HU_r} = \frac{\Delta M^{\nu}_{cum} - \sum_{n=1}^{r-1} F^{HU_n}\left(y^{HU_r} - y^{HU_n}\right)}{y^{\nu} - y^{HU_r}} - \sum_{n=1}^{r-1} F^{HU_n} \tag{13.16}$$

where n denotes the index for the nth external hydrogen source ($n < r$).

The product of the purifier is considered as an external hydrogen source. The product impurity ($y^{\text{prod}} = 0.1$) fulfills the condition ($y^{\text{prod}} < y^{\text{pinch}}_{\text{HU}}$) and thus the flowrate of hydrogen utility can be further reduced with the introduction of the product of the purifier. All the possible flowrates of the product of the purifier at an impurity level greater than and equal to the product impurity (i.e., $y^{\nu} \geq 0.1$) can be calculated via solving Eq. (13.15). The maximum value (113,890 Nm^3/h) in the seventh column of Table 13.2 may be determined as the optimal flowrate of the product of the purifier and its feasibility should be checked in Step 8.

Step 7: Waste hydrogen streams identification: Waste hydrogen streams discharged from the network are identified. On the pinch (the impurity is 0.25), the accumulated hydrogen flowrate is 85,418 Nm^3/h. It can be considered as an internal hydrogen source with an impurity of 0.25. Then, for each impurity interval above 0.25 (i.e., $y^{\nu} > y^{\text{pinch}}$), the required flowrates can be calculated via Eq. (13.17) and all the possible flowrates for $F^{\text{pinch}}_{\text{above}}$ are listed in the eighth column of Table 13.2 and the maximum value (68,808 Nm^3/h) is the targeted minimum flowrate that would be supplied for the region above an impurity of 0.25. Therefore, only 68,808 Nm^3/h of hydrogen source at an impurity of 0.25 needs to be distributed to the system, and the surplus flowrate 16,610 Nm^3/h (=85,418 − 68,808 Nm^3/h) is identified as the waste hydrogen stream WH1 (0.25). Similarly, the waste hydrogen streams (WH2 and WH3) are identified and the flowrates are shown in the final column of Table 13.2. Their corresponding impurities (the values in the 11th column) are impurities

of identified waste hydrogen streams. The identified waste hydrogen streams are discharged to the fuel system in the direct reuse/recycle scheme. However, for the purification reuse/recycle scheme, the identified waste hydrogen streams are either allocated to the purifier as its feed or discharged into the fuel system.

$$F_{\text{above}}^{\text{pinch}} = \frac{\Delta M_{cum}^{\nu} - \Delta M_{cum}^{\text{pinch}}}{y^{\nu} - y^{\text{pinch}}} \quad \forall y^{\nu} > y^{\text{pinch}} \tag{13.17}$$

Step 8: Mass balance check: The mass balance for a system with purification reuse/recycle shall be performed to check the feasibility. The procedure can be divided into three substeps.

Substep 1: Calculate the values for F^{HU}, F^{prod}, $F_{\text{sys}}^{\text{resd}}$, $F_{\text{loss}}^{\text{sys}}$, $F_{\text{fuel}}^{\text{sys}}$, F^{feed}, and $y_{\text{H}_2}^{\text{feed}}$.

The maximum value in the sixth column of Table 13.2 within the impurity region ($0.05 < y \leq 0.1$) is 0 t/h, which is identified as the minimum flowrate of hydrogen utility ($F^{\text{HU}} = 0\,\text{Nm}^3/\text{h}$) with purification reuse/recycle. The maximum value in the seventh column within the concentration region ($0.1 < y \leq 0.45$) is targeted as the minimum flowrate of the product of the purifier that is allocated to the direct reuse/recycle system ($F^{\text{prod}} = 113{,}890\,\text{Nm}^3/\text{h}$). The total net flowrate for the system ($F_{\text{loss}}^{\text{sys}}$) is calculated in Step 2 as $62{,}349\,\text{Nm}^3/\text{h}$. The residual of the purifier with high impurity is not allowed to be reused by any hydrogen sinks and $F_{\text{sys}}^{\text{resd}}$ is assumed to be zero. In order to maximize the recovery, all the waste hydrogen streams are assumed to be fed to the purifier and thus $F_{\text{fuel}}^{\text{sys}}$ is assumed to be zero. Next, F^{feed} can be calculated as $51{,}542\,\text{Nm}^3/\text{h}$ via solving Eq. (13.9), and this is greater than the capacity of the purifier. It is infeasible and the infeasibility will be removed in substep 3. The total flowrate of all the identified waste hydrogen streams ($\sum F^{\text{WH}}$) is calculated as $51{,}542\,\text{Nm}^3/\text{h}$. The difference between $\sum F^{\text{WH}}$ and F^{feed} is calculated to validate the assumption that all the waste hydrogen streams are assigned as the feed of the purifier. Next, the purity of the mixed waste hydrogen stream specifies the feed purity for the purifier and $y_{\text{H}_2}^{\text{feed}}$ is calculated as 0.734, which is less than the pinch purity. The values for F^{HU}, F^{prod}, $F_{\text{sys}}^{\text{resd}}$, $F_{\text{loss}}^{\text{sys}}$, $F_{\text{fuel}}^{\text{sys}}$, F^{feed}, and $y_{\text{H}_2}^{\text{feed}}$ are marked in bold in Table 13.2.

Substep 2: Calculate the values for $F^{\text{prod}}y_{\text{H}_2}^{\text{prod}}$, $F^{\text{feed}}y_{\text{H}_2}^{\text{feed}}$, F^{feed}, $F^{\text{resd}}y_{\text{H}_2}^{\text{resd}}$ and ΔF^{feed}.

$F^{\text{prod}}y_{\text{H}_2}^{\text{prod}}$ can be calculated as $102{,}501\,\text{Nm}^3/\text{h}$ with the given $y_{\text{H}_2}^{\text{prod}} = 0.90$ and determined value $F^{\text{prod}} = 113{,}890\,\text{Nm}^3/\text{h}$. $F^{\text{feed}}y_{\text{H}_2}^{\text{feed}}$ is next calculated as $113{,}890\,\text{Nm}^3/\text{h}$ via solving Eq. (13.5). Next F^{feed} is determined as $155{,}218\,\text{Nm}^3/\text{h}$ ($=113{,}890\,\text{Nm}^3/\text{h}/0.734$). Next $F^{\text{resd}}y_{\text{H}_2}^{\text{resd}}$ is calculated as $11{,}389\,\text{Nm}^3/\text{h}$ via solving Eq. (13.4). The difference between two F^{feed}s (ΔF^{feed}) is determined as $103{,}677\,\text{Nm}^3/\text{h}$. The values for $F^{\text{prod}}y_{\text{H}_2}^{\text{prod}}$, $F^{\text{feed}}y_{\text{H}_2}^{\text{feed}}$, F^{feed}, $F^{\text{resd}}y_{\text{H}_2}^{\text{resd}}$ and ΔF^{feed} are marked in *italic* in Table 13.2.

Substep 3: Check the feasibility and determine the optimal targets.

Note that ΔF^{feed} is $103{,}677\,\text{Nm}^3/\text{h}$ and it indicates the infeasibility of the results. The optimal and feasible target for ΔF^{feed} should be zero. The other

variables in *substeps 1 and 2* can be related with the variable F_{HU} via the equations mentioned in *substeps 1 and 2*. The Excel Goal Seek feature is utilized to determine the optimal target ΔF^{feed} by changing the value of F^{HU}. In the Excel Goal Seek control box, ΔF^{feed} is set to be the target value of zero and the value of F^{HU} is set to be altered. Once we click the "OK" button on the Excel Goal Seek control box, ΔF^{feed} achieves zero and the values of all other variables are changed to the new results shown in Table 13.3. The optimal flowrate of hydrogen utility with a purification reuse/recycle scheme is determined to be 70,220 Nm^3/h, which is 15,197 Nm^3/h less than that (85,418 Nm^3/h) with a direct reuse/recycle scheme. The optimal flowrate of the product of the purifier is determined to be 20,263 Nm^3/h with the minimum flowrate of hydrogen utility. The optimal flowrate of the feed of the purifier is 28,135 Nm^3/h with an optimal feed purity of 0.72 (i.e., the impurity is 0.28). This indicates that the optimal feed impurity of the purifier is not necessarily to be the pinch impurity as assumed in the literature (2006).

As shown in Fig. 13.7, the first segment of HSL can be constructed within the impurity intervals of 0.05 and 0.1 with its inverse slope corresponding to 70,220 Nm^3/h (F^{HU}). The section of LCC above it is considered as Region 1, where only hydrogen utility is allocated to fulfill the requirement. The second segment of HSL can be constructed with the impurity intervals of 0.1 and 0.45 with its inverse slope corresponding to 90,484 Nm^3/h (=70,220 + 20,263 Nm^3/h). The section of LCC above it is considered as Region 2, where F^{HU} and F^{prod} are referenced to remove the load of this region.

Step 9: Hydrogen network design: Design the hydrogen network via the nearest neighbors algorithm (NNA) (Prakash and Shenoy, 2005). Fig. 13.8 illustrates one optimal hydrogen network with purification reuse/recycle.

In this section, IPT is introduced in detail for the determination of the optimal targets for a hydrogen network with purification reuse/recycle. With the introduction of the product stream of purifier, the flowrate of hydrogen utility can be reduced from 85,418 to 70,220 Nm^3/h. It is worth mentioning that IPT can locate the exact optimal feed impurity of the purifier, which is greater than or equal to the pinch impurity.

13.4 DESIGN OF HYDROGEN NETWORK VIA MATHEMATICAL PROGRAMMING APPROACH

The main feature of the insight-based pinch technique is that the pinch technique can be used to determine the flowrate of hydrogen utility intuitively. However, it has certain difficulties in handling the automated optimal synthesis of a hydrogen network with pressure constraints, multiple impurities, and the annualized cost as the objectives. It leads to the development of superstructure-based mathematical programming approaches. Hallale and Liu (2001) firstly proposed a superstructure embedded with hydrogen sources, sinks, and compressors, and then optimized it mathematically to maximize

TABLE 13.3 Implementation of IPT for Case 1 With Purification Reuse/Recycle (Optimal Solution) (Deng et al., 2015).

Purity (Fraction)	Impurity (Fraction)	Net Flowrate (Nm^3/h)	Net Load (Nm^3/h)	Cumulative Load (Nm^3/h)	Hydrogen Utility (Nm^3/h)	Flowrate for Purification Product (Nm^3/h)	Flowrate Above Pinch (Nm^3/h)	Flowrate Above Pinch (Nm^3/h)	Flowrate Above Pinch (Nm^3/h)	Flowrate for Waste Hydrogen Stream (Nm^3/h)
0.95	0.05			0	0.00					
		0	0							
0.9	0.1			0	70,220					
		0	0							
0.8671	0.1329			0	0	−1,768,904				
		93,306	2917							
0.8358	0.1642			2917	25,549	−79,472				
		175,962	1783							
0.8257	0.1743			4700	37,808	−54,221				
		215,127	5526							
0.8	0.2			10,226	68,175	−3068				
		137,146	6857							
0.75	0.25			17,084	85,418	20,263				21,675
		55,995	1512							

0.7230	0.277			18,596	81,917	15,001	55,995			
		68,467	562							
0.7148	0.2852			19,158	81,448	14,259	58,901			
		74,193	4807							
0.65	0.35			23,964	79,881	11,593	68,808			2619
		66,189	3309							
0.6	0.4			27,274	77,925	8989	67,935	66,189		3840
		62,349	3117							
0.55	0.45			30,391	75,978	6580	66,538	64,269	62,349	

Eqs. (13.12), (13.11)	$F^{feed}y_{H_2}{}^{feed}$	$F^{prod}y_{H_2}{}^{prod}$	$F^{resd}y_{H_2}{}^{resd}$	$y_{H_2}{}^{feed}$	F^{feed}	$\sum F^{WH}$	ΔF^{feed}
	20,263	***18,237***	***2026***	***0.72***	***28,135***	***28,135***	***0***
Eq. (13.9)	F_{HU}	F^{prod}	F_{sys}^{resd}	F_{loss}^{sys}	F^{feed}	F_{fuel}^{sys}	$\sum F^{WH} - F^{feed}$
	70,220	20,263	0	62,349	28,135	0	0

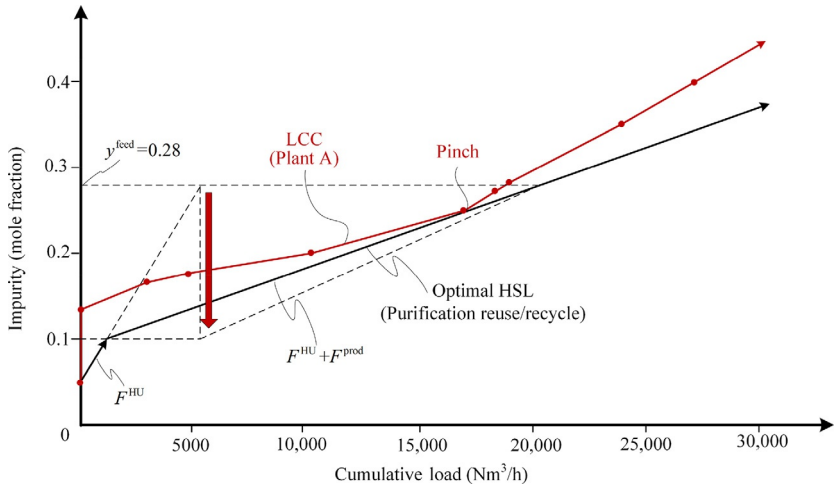

FIG. 13.7 LCC and optimal HSL with purification reuse/recycle (Deng et al., 2015).

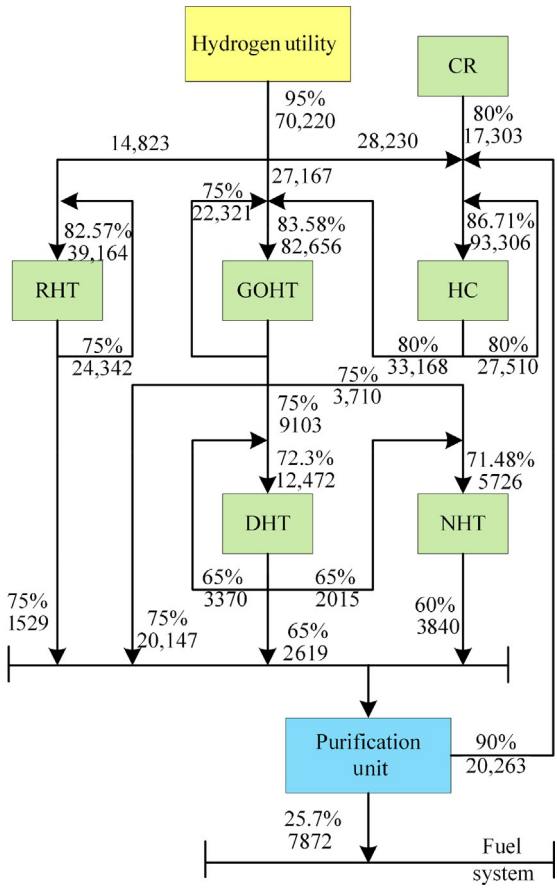

FIG. 13.8 Optimal network for case 1 with purification reuse/recycle (Deng et al., 2015).

hydrogen recovery in the clean fuels production process. Many other mathematical programming approaches were developed and they can be found in the review (Marques et al., 2017). In this section, a mathematical model (Deng et al., 2014) for the synthesis of refinery hydrogen networks is introduced and one case is analyzed to illustrate the application of the introduced model.

13.4.1 Problem Statement

Given a set of internal hydrogen sources (or so-called process hydrogen sources) with the total number of NSR, for each internal hydrogen source ($s \in NSR$) with specified flow rate (FSR_s), find the concentration of the cth component ($y_{s,c}^{out}$) ($c \in NC$), and pressure (PSR_s). With the appropriate placement of a number of gas compressors ($i \in NI$), those hydrogen sources can be allocated with a set of hydrogen sinks. With a number of hydrogen sinks (NSK), each sink ($k \in NSK$) has its own flow rate requirement (FK_k^{in}), minimum hydrogen purity, maximum allowable inlet concentration of impurity, and pressure specification (PK_k^{in}). In addition, a number of external hydrogen sources ($u \in NHU$), so-called hydrogen utilities, from hydrogen plants would be utilized to compensate the internal hydrogen source to fulfill the requirements of hydrogen sinks. Besides, in order to reduce the flow rate of hydrogen utility, a number of purifiers ($p \in NP$) can be placed to upgrade the quality of certain internal hydrogen sources for further utilization by hydrogen sinks. The superstructure of the problem, embedded with potential configurations of interest is shown in Fig. 13.9.

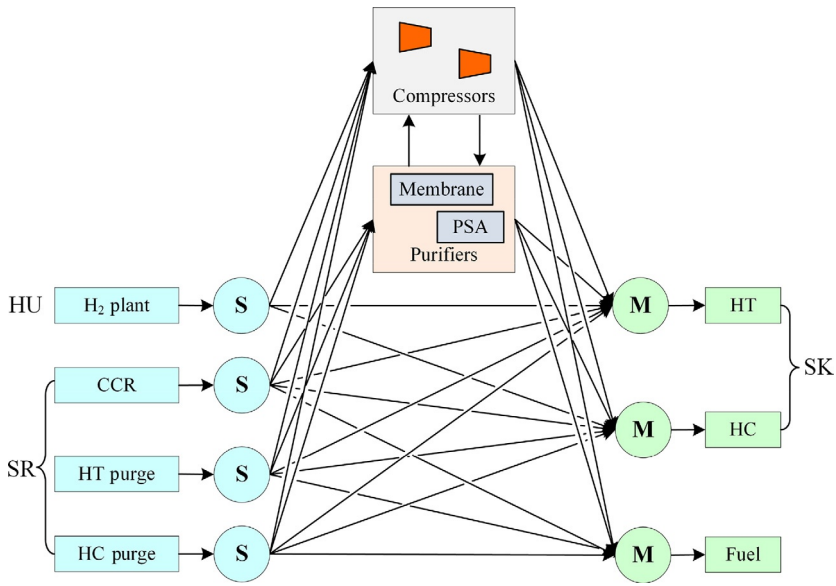

FIG. 13.9 Superstructure for the synthesis of a hydrogen network (Deng et al., 2014).

13.4.2 Mathematical Model

The mathematical formulations (Deng et al., 2014) for the superstructure shown in Fig. 13.9 can be presented as follows.

13.4.2.1 Formulations Related to the uth Hydrogen Utility

A hydrogen production process, such as steam reforming of natural gas, serves as hydrogen utility in the refinery plant. In addition, several available external hydrogen sources from an ethylene plant, fertilizer plant, and coal gasification section would be possible hydrogen utilities. The pressure for the hydrogen utility would not fulfill the pressure requirement of hydrogen sinks and hydrogen compressors would be installed to raise the pressure. Typically, due to the high quality of the hydrogen utility, it would not be allocated to purifiers. In addition, the hydrogen utility would not be allowed to discharge to the fuel system.

The gas stream from hydrogen utility can be allocated to the hydrogen sink if the inlet conditions are satisfied or be allocated to the *i*th hydrogen compressor to lift its pressure to fulfill the requirement of hydrogen sinks or purifiers. The flow rate balance is made on the splitting node after the *u*th hydrogen utility,

$$FHU_u = \sum_{k \in NSK} FUK_{u,k} + \sum_{i \in NI} FUI_{u,i} \quad \forall u \in NHU \tag{13.18}$$

Note that the gas flow rate for the *u*th hydrogen utility cannot exceed its maximum capacity,

$$FHU_u \leq \mathrm{FHU}_{\mathrm{u}}^{\mathrm{UB}} \tag{13.19}$$

13.4.2.2 Formulations Related to the sth Hydrogen Source

The continuous catalytic reforming (CCR) process is the typical hydrogen source in a refinery. In addition, the purges of hydrogen treating and hydrogen cracking processes contain a certain amount of hydrogen. They are categorized as internal hydrogen sources and can be reused by other hydrogen sinks (hydrogen treating and hydrogen cracking processes). Alternatively, they may be allocated to purifiers (PSA or Membrane) to upgrade the quality and then assigned to hydrogen sinks. The compressors can be installed to lift the pressure of the hydrogen sources. The surplus hydrogen sources with low purity of hydrogen can be discharged into the fuel system.

The flow rate balance can be made for the splitting node after the *s*th hydrogen source,

$$FSR_s = \sum_{k \in NSK} FSK_{s,k} + \sum_{i \in NI} FSI_{s,i} + \sum_{p \in NP} FSP_{s,p} + \sum_{f \in NF} FSF_{s,f} \quad \forall s \in NSR \tag{13.20}$$

The gas flow rate for the sth hydrogen source cannot exceed its upper bounds,

$$FSR_s \leq \mathrm{FSR}_{\mathrm{s}}^{\mathrm{UB}} \tag{13.21}$$

13.4.2.3 Formulations Related to the ith Compressor

The inlet gas stream of the ith compressor could come from hydrogen utility, hydrogen source, product of purifiers or other compressors.

The flow rate balance can be made for the mixing node before the ith compressor,

$$FI_i^{in} = \sum_{u \in NHU} FUI_{u,i} + \sum_{s \in NSR} FSI_{s,i} + \sum_{p \in NP} FPI_{p,i}^{prod} + \sum_{\substack{i' \neq i \\ i' \in NI}} FII_{i',i} \quad \forall i \in NI \tag{13.22}$$

In addition, the mass balance for the cth component can be made for the mixing node before the ith compressor,

$$FI_i^{in} \cdot y_{i,c}^{in} = \sum_{u \in NHU} FUI_{u,i} \cdot y_{u,c}^{out} + \sum_{s \in NSR} FSI_{s,i} \cdot y_{s,c}^{out} + \sum_{\substack{i' \neq i \\ i' \in NI}} FII_{i',i} \cdot y_{i',c}^{out} \quad \forall i \in NI \ \forall c \in NC \tag{13.23}$$

The flow rate balance and mass balance for the cth component are made around the outlet and inlet of the ith compressor,

$$FI_i^{out} = FI_i^{in} \quad \forall i \in NI \tag{13.24}$$

$$y_{i,c}^{out} = y_{i,c}^{in} \quad \forall i \in NI \ \forall c \in NC \tag{13.25}$$

The outlet gas stream of the ith compressor could be allocated to hydrogen sinks, the purifier, or other compressors. The flow rate balance can be made for the splitting node after the ith compressor,

$$FI_i^{out} = \sum_{k \in NSK} FIK_{i,k} + \sum_{p \in NP} FIP_{i,p} + \sum_{\substack{i' \neq i \\ i' \in NI}} FII_{i,i'} \quad \forall i \in NI \tag{13.26}$$

In addition, the inlet gas flow rate must not exceed its maximum flow rate capacity for the existing compressor,

$$FI_i^{in} \leq \mathrm{FI}_i^{\mathrm{in,UB}} \quad \forall i \in NI_{\mathrm{exist}} \tag{13.27}$$

13.4.2.4 Formulations Related to the pth Purifier

The inlet gas stream for the purifier would include gas streams from hydrogen sources and compressors. Typically, the purifier (PSA and Membrane) has two

outlets: product and residual. The product of higher hydrogen purity can be allocated to hydrogen sinks or compressors, if necessary. However, the residual with low hydrogen purity is typically assigned to the fuel system.

The flow rate balance and component mass balance are made for the mixing node before the pth purifier,

$$FP_p^{in} = \sum_{s \in NSR} FSP_{s,p} + \sum_{i \in NI} FIP_{i,p} \quad \forall p \in NP \tag{13.28}$$

$$FP_p^{in} \cdot y_{p,in}^{in} = \sum_{s \in NSR} FSP_{s,p} \cdot y_{u,c}^{out} + \sum_{i \in NI} FIP_{i,p} \cdot y_{i,c}^{out} \quad \forall p \in NP \; c \in NC \tag{13.29}$$

The flow rate balance and component mass balance are made around the pth purifier,

$$FP_p^{in} = FP_p^{prod} + FP_p^{resd} \quad \forall p \in NP \tag{13.30}$$

$$FP_p^{in} \cdot y_{p,c}^{in} = FP_p^{prod} \cdot y_{p,c}^{prod} + FP_p^{resd} \cdot y_{p,c}^{resd} \quad \forall p \in NP \; c \in NC \tag{13.31}$$

The cth component contained in the product divided by that contained in the feed of the pth purifier is defined as the recovery ratio ($RR_{p,c}$). Typically, the hydrogen recovery ratio is specified for each purifier.

$$FP_p^{prod} \cdot y_{p,c}^{prod} = RR_{p,c} \cdot FP_p^{in} \cdot y_{p,c}^{in} \quad \forall p \in NP \; c \in NC \tag{13.32}$$

The flow rate balance is made on the splitting node after the pth purifier,

$$FP_p^{prod} = \sum_{k \in NSK} FPK_{p,k}^{prod} + \sum_{i \in NI} FPI_{p,i}^{prod} \quad \forall p \in NP \tag{13.33}$$

$$FP_p^{resd} = \sum_{f \in NF} FPF_{p,f}^{resd} \quad \forall p \in NP \tag{13.34}$$

13.4.2.5 Formulations Related to the kth Hydrogen Sink

The inlet gas stream for the kth hydrogen sink would be supplied by hydrogen utility, hydrogen sources, purifiers, and compressors.

The flow rate and component mass balance are made on the mixing node before the kth hydrogen sink,

$$\mathrm{FK}_k^{\mathrm{in}} = \sum_{u \in NHU} FUK_{u,k} + \sum_{s \in NSR} FSK_{s,k} + \sum_{p \in NP} FPK_{p,k}^{prod} + \sum_{i \in NI} FIK_{c,k} \quad \forall k \in NSK \tag{13.35}$$

$$\mathrm{FK}_k^{\mathrm{in}} \cdot y_{k,c}^{in} = \sum_{u \in NHU} FUK_{u,k} \cdot y_{u,c}^{out} + \sum_{s \in NSR} FSK_{s,k} \cdot y_{s,c}^{out} + \sum_{p \in NP} FPK_{p,k}^{prod} \cdot y_{p,c}^{prod} + \sum_{i \in NI} FIK_{i,k} \cdot y_{i,c}^{out} \quad \forall k \in NSK \; c \in NC \tag{13.36}$$

The inlet hydrogen purity must be higher than its lower bound specified by the hydrogen sink,

$$y_{k,c}^{in} \geq y_{k,c}^{\text{in,LB}} \quad \forall c = \{\text{H}_2\} \tag{13.37}$$

13.4.2.6 Formulations Related to the Fuel System

The surplus internal hydrogen source and the residual gas stream of the purifier would be sent to the fuel system. The flow rate and component mass balance are made on the mixing node before the fuel system,

$$FF^{in} = \sum_{s \in NSR} FSF_s + \sum_{p \in NP} FPF_p^{resd} \tag{13.38}$$

$$FF^{in} \cdot y_{f,c}^{in} = \sum_{s \in NSR} FSF_s \cdot y_{s,c}^{out} + \sum_{p \in NP} FPF_p^{resd} \cdot y_{p,c}^{resd} \quad \forall c \in NC \tag{13.39}$$

Note that, the inlet flow rate of the fuel system (FF^{in}) and inlet concentration for the cth component ($y_{f,\,c}^{in}$) are two variables and they make the term ($FF^{in} \cdot y_{f,\,c}^{in}$) a bilinear term. To reduce the number of bilinear terms in the mathematical model, Eq. (13.39) is not included in the constraints, but it will be solved after the optimization.

13.4.2.7 Connection and Pressure Constraints

The binary variables $z_{a,\,b}$ are introduced to indicate the connection status between supplier (hydrogen utility, hydrogen source, outlet of compressor, product, and residual of purifier) and receiver (hydrogen sink, inlet of compressor, inlet of purifier, fuel system). The necessary and sufficient condition for a connection extension is that the flow rate is nonzero. The flow rates serving as continuous variables are related with binary variables by Eq. (13.40),

$$\begin{aligned}
&F_{a,b} - z_{a,b} \cdot \text{F}_{\text{a,b}}^{\text{UB}} \leq 0 \\
&F_{a,b} + (1 - z_{a,b}) \cdot \text{F}_{\text{a,b}}^{\text{UB}} \geq \text{F}_{\text{a,b}}^{\text{LB}} \\
&z_{a,b} \in \left\{ \begin{array}{l} zUK_{u,k}, zUP_{u,p}, zUI_{u,i} \\ zSK_{s,k}, zSP_{s,p}, zSI_{s,i}, zSF_{s,f} \\ zPK_{p,k}^{prod}, zPI_{p,i}^{prod}, zPF_{p,f}^{resd} \\ zIK_{i,k}, zIP_{i,p}, zII_{i,i'} \end{array} \right\} \\
&F_{a,b} \in \left\{ \begin{array}{l} FUK_{u,k}, FUP_{u,p}, FUI_{u,i} \\ FSK_{s,k}, FSP_{s,p}, FSI_{s,i}, FSF_{s,f} \\ FPK_{p,k}^{prod}, FPI_{p,i}^{prod}, FPF_{p,f}^{resd} \\ FIK_{i,k}, FIP_{i,p}, FII_{i,i'} \end{array} \right\}
\end{aligned} \tag{13.40}$$

where $F^{UB}_{a,b}$ and $F^{LB}_{a,b}$ are the upper and lower bounds for the flow rate variable $F_{a,b}$.

Once the pressure level of a hydrogen sink or purifier is higher than that of a hydrogen source, the hydrogen source cannot be fed to the hydrogen sink or purifier directly and the hydrogen compressor is necessary to upgrade the pressure level of the hydrogen source. It indicates that the flow rate from the hydrogen source to the sink or purifier with higher pressure level equals zero. The condition can be fulfilled by Eqs. (13.40), (13.41).

$$\begin{aligned}
&(P_b - P_a)\cdot F_{a,b} \le 0\\
&P_a \in \left\{\mathrm{PHU}^{\mathrm{out}}_{\mathrm{u}}, \mathrm{PSR}^{\mathrm{out}}_{\mathrm{s}}, \mathrm{P}^{\mathrm{prod}}_{\mathrm{p}}, \mathrm{P}^{\mathrm{resd}}_{\mathrm{p}}, \mathrm{PI}^{\mathrm{out}}_{\mathrm{i}}\right\}\\
&P_b \in \left\{\mathrm{PK}^{\mathrm{in}}_{\mathrm{k}}, \mathrm{PP}^{\mathrm{in}}_{\mathrm{p}}, \mathrm{PI}^{\mathrm{in}}_{\mathrm{i}}\right\}\\
&F_{a,b} \in \begin{Bmatrix} FUK_{u,k}, FUP_{u,p}, FUI_{u,i}\\ FSK_{s,k}, FSP_{s,p}, FSI_{s,i}, FSF_{s,f}\\ FPK^{prod}_{p,k}, FPI^{prod}_{p,i}, FPF^{resd}_{p,f}\\ FIK_{i,k}, FIP_{i,p}, FII_{i,i'} \end{Bmatrix}
\end{aligned} \tag{13.41}$$

The pressure for the mixed stream of hydrogen sources is determined by the minimum pressure of the hydrogen sources associated with the mixed stream.

$$P^{\mathrm{mix}} = \min\{\mathrm{P_a}\} \quad \forall \mathrm{P_a} \in \left\{\mathrm{PHU}^{\mathrm{out}}_{\mathrm{u}}, \mathrm{PSR}^{\mathrm{out}}_{\mathrm{s}}, \mathrm{P}^{\mathrm{prod}}_{\mathrm{p}}, \mathrm{P}^{\mathrm{resd}}_{\mathrm{p}}, \mathrm{PI}^{\mathrm{out}}_{\mathrm{i}}\right\} \tag{13.42}$$

The total number of connections (N_{total}) is an important parameter for the demonstration of network complexity. It is the summation of all the connection variables, and given as Eq. (13.43).

$$\begin{aligned}
N_{total} = &\sum_u \sum_k zUK_{u,k} + \sum_u \sum_p zUP_{u,p} + \sum_u \sum_i zUI_{u,i}\\
&+ \sum_s \sum_k zSK_{s,k} + \sum_s \sum_p zSP_{s,p} + \sum_s \sum_i zSI_{s,i} + \sum_s \sum_i zSF_{s,f}\\
&+ \sum_p \sum_k zPK^{prod}_{p,k} + \sum_p \sum_i zPI^{prod}_{p,i} + \sum_p \sum_f zPF^{resd}_{p,f}\\
&+ \sum_i \sum_k zIK_{i,k} + \sum_i \sum_p zIP_{i,p} + \sum_i \sum_{i'} zII_{i,i'}
\end{aligned} \tag{13.43}$$

13.4.2.8 Objective Functions

The flow rate of hydrogen utility is strongly related to the capacity of the hydrogen plant and its operating cost. Therefore, the objective function can be formulated to minimize the consumption of hydrogen utility.

$$\min FHU = \sum_{u \in NHU} FHU_u \tag{13.44}$$

In addition, the minimum total number of connections can be determined by setting an upper bound. The upper bound can be reduced one by one until the optimal flow rate of hydrogen utility tends to increase. The corresponding total number of connections is considered as the minimum target.

Besides, the total annualized cost (TAC) can also be employed as an optimization objective. It can be found in the literature (Deng et al., 2014).

13.4.3 Case Study

Fig. 13.10 shows the current hydrogen network for case 2, which is adopted from the base case of Elkamel et al. (2011)). As shown, the existing fresh hydrogen consumption from the hydrogen plant is reported as 89,280 Nm^3/h (80 MMscfd) (Elkamel et al., 2011). The current process data for this example are listed in Table 13.4. As shown, there are five hydrogen consuming processes, namely, hydrocracker unit (HCU), gas oil hydrotreater (GOHT), residue hydrotreater (RHT), diesel hydrotreater (DHT), and naphtha hydrotreater (NHT). The inlets for these hydrogen consumers serve as internal hydrogen sinks and their outlets would be considered as internal hydrogen sources.

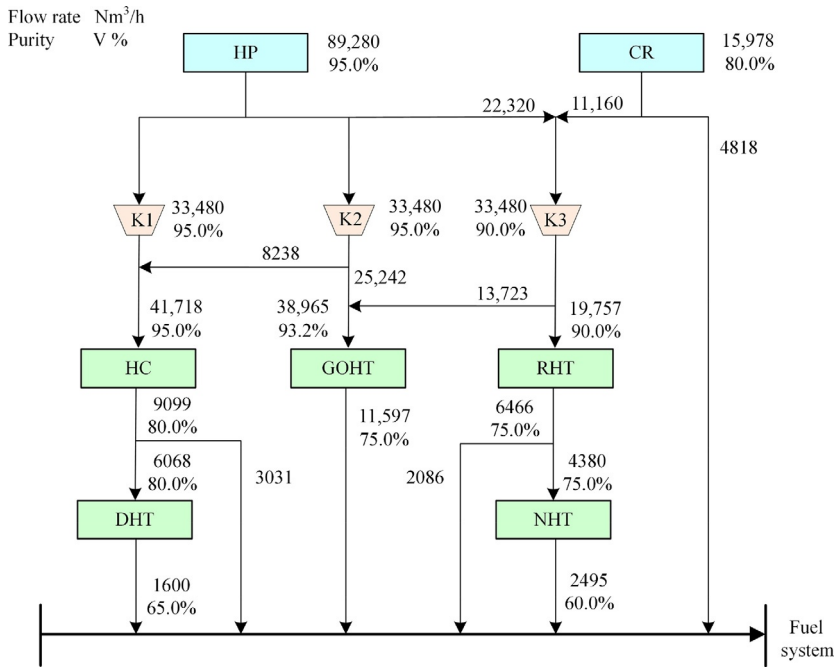

FIG. 13.10 Current hydrogen network for Case 2 (Elkamel et al., 2011).

TABLE 13.4 Limiting Data for Case 2

Sources	Sinks						Current Flow Rate (Nm^3/h)	Maximum Flow Rate (Nm^3/h)	Purity (V% H_2)	Pressure (MPa)
	HCU	GOHT	RHT	DHT	NHT	Fuel				
HP	41,718	38,965	8597				89,280	89,280	95	2.069
CRU			11,160			4818	15,978	16,182	80	2.069
HCU				6068		3031	9099	9099	80	8.276
GOHT						11,597	11,597	11,597	75	2.414
RHT					4380	6466	10,846	10,846	75	2.759
DHT						1600	1600	1600	65	2.414
NHT						2495	2495	2495	60	1.379
Flow rate (Nm^3/h)	41,718	38,965	19,757	6068	4380	30,008				
Purity (V % H_2)	95.00	93.20	90.00	80.00	75.00					
Pressure (MPa)	13.79	3.448	4.138	3.448	2.069					

The purity and pressure requirements for the sinks and the purity and pressure conditions for the sources are listed in Table 13.4. Note that all the hydrogen consumers have internal recycle compressors. The recycle hydrogen streams would not serve as hydrogen sources. In addition, a catalytic reforming unit (CRU) is an internal hydrogen source with specified hydrogen purity of 80%, outlet pressure of 2.069 MPa, and maximum capacity of 16,182 Nm^3/h. Its maximum capacity is assumed in this paper according to the optimized results in the literature (Elkamel et al., 2011). In order to reduce the operating cost for the hydrogen plant, the internal hydrogen sources should be fully utilized before the hydrogen utility from the hydrogen plant is considered. In this case, the hydrogen utility is specified with a hydrogen purity content of 95%, outlet pressure of 2.069 MPa, and maximum capacity of 89,280 Nm^3/h. Besides, the fuel system operates at low pressure (1.379 MPa), which would receive unused internal hydrogen sources. The case will be used to investigate the influences of the placement of the purifier on the consumption of hydrogen utility.

In order to reduce the consumption of hydrogen utility further, the purification unit (PSA) is incorporated into the hydrogen network to upgrade the quality of internal hydrogen sources and the product of the PSA will be assigned to hydrogen sinks if the pressure requirement is fulfilled.

To model the placement of compressor and purifier, the objective function is selected as Eq. (13.44) and it is subjected to the constraints in Eqs. (13.18)–(13.38) and connection constraint (13.40) and pressure constraint (13.41). Note that the connection constraint (13.40) and the bilinear terms ($FI_i^{in} \cdot y_{i,c}^{in}$) and ($FP_p^{in} \cdot y_{p,c}^{in}$) contained in Eqs. (13.23), (13.29) make the model a MINLP problem. It is solved in GAMS software (Rosenthal, 2010) using DICOPT as solver (based on the PC specification: Intel Core i3-2100 CPU 3.10 GHz, 4 GB RAM). Note that the solver CPLEX is defined to solve MIP problems as well as KNITRO for NLP problems.

The process data for the purification unit PSA are assumed in this paper. The inlet pressure for PSA is set to 2.069 MPa. The pressure for the product of PSA is assumed to be 2.069 MPa and the slight pressure drop is neglected. The hydrogen purity for its product is given as 95% and the hydrogen recovery is defined as 90%. Besides, the pressure for its residue is set to 1.379 MPa. The maximum inlet flow rate for PSA is assumed to be 35,712 Nm^3/h. Once the above data, as well as the data listed in Tables 13.4 and 13.5, were input to the model, the model was solved in 0.02 CPUs and the optimal flow rate of hydrogen utility was found to be 72,444 Nm^3/h with a minimum number of connections of 20. The optimized results are listed in Table 13.6 and Fig. 13.11 shows the optimized hydrogen network with the placement of compressors and purifier. As shown, the product of PSA is assigned to compressor K1 and then allocated to hydrogen sinks. The total inlet flow rate and purity for PSA is determined as 23,235 Nm^3/h and 76.022%.

In order to investigate the influence of the feed hydrogen purity for PSA on the hydrogen utility, feed hydrogen purity for PSA is given in the region [70, 80]

TABLE 13.5 Process Data for the Make-Up Hydrogen Compressor

Compressor	Inlet Pressure (MPa)	Discharge Pressure (MPa)	Maximum Capacity (Nm^3/h)
K1	2.069	13.79	35,154
K2	2.069	13.79	35,154
K3	2.069	4.138	35,154

with an increment of one. Fig. 13.12 shows the variation tendencies of feed flow rate of PSA, optimum flow rate of hydrogen utility, and minimum total number of connections with the increase of feed hydrogen purity for PSA. As shown in Fig. 13.12, the minimum flow rate of hydrogen utility is 72,444 Nm^3/h with 76.022% of feed hydrogen purity for the product of PSA. The feed flow rate of PSA increases with the increment of feed hydrogen purity of PSA. The minimum total number of connections is kept at 20 until the feed hydrogen purity of PSA reaches 76.022%. Once the feed hydrogen purity of PSA is less than 76.022%, the minimum total number of connections will be greater than 20 and fluctuate with the increase of the feed hydrogen purity of PSA. And the minimum total number of connections is kept at 22 when the feed hydrogen purity of PSA is greater than 76.022%. For this case, the minimum flow rate of hydrogen utility is targeted to be 72,444 Nm^3/h with 20 connections and 76.022% of feed hydrogen purity of PSA and the feed flow rate of PSA is determined as 23,235 Nm^3/h.

13.5 CONCLUSION

In this chapter, both the Pinch technique and mathematical programming approaches are introduced for the synthesis of a hydrogen network with a purification unit. A generalized Improved Problem Table (IPT) is presented and mass balance equations are incorporated to determine the optimal targets (i.e., the optimal flowrates of hydrogen utility and product of the purifier, optimal feed impurity of purifier). The optimal feed impurity of the purifier is greater than or equal to the pinch impurity with the direct reuse/recycle scheme. The limiting composite curves (LCCs) and optimal hydrogen supply lines (HSL) are plotted vividly to show the insights of the proposed approach. Next, a superstructure-based optimization model is introduced and a comprehensive superstructure is embedded with hydrogen utility, process hydrogen sources, hydrogen sinks, fuel system, compressor, purifier, and all the feasible interconnections between them. The optimization results show that the optimal flow rate of hydrogen utility will be increased with the reduction of the total number of

TABLE 13.6 Optimum Results for Case 2 With the Placement of Compressors (Purification Reuse/Recycle) (Deng et al., 2014)

Sources	Sinks									Fuel System	Optimized Flow Rate (Nm^3/h)	Maximum Flow Rate (Nm^3/h)	Purity (V% H_2)	Pressure (MPa)
	HCU	GOHT	RHT	DHT	NHT	K1	K2	K3	PSA					
HP						16,914	28,606	26,924			72,444	89,280	95	2.069
CRU								8230	7952		16,182	16,182	80	2.069
HCU			3031	6068							9099	9099	80	8.276
GOHT					4380				7217		11,597	11,597	75	2.414
RHT									6466		6466	6466	75	2.759
DHT									1600		1600	1600	65	2.414
NHT										2495	2495	2495	60	1.379
K1	13,112	18,993	1544								33,649	35,154	95	13.79
K2	28,606										28,606	35,154	95	13.79
K3		19,972	15,182								35,154	35,154	91.488	4.138
PSA Product						16,735							95	2.069
PSA Residue										6501			27.171	1.379
Flow rate (Nm^3/h)	41,718	38,965	19,757	6068	4380	33,649	28,606	35,154	23,235	8996			36.277	
Purity (V % H2)	95.00	93.20	90.00	80.00	75.00	95.00	95.00	91.488	76.022	36.277				
Pressure (MPa)	13.79	3.448	4.138	3.448	2.069	2.069	2.069	2.069	2.069	1.379				

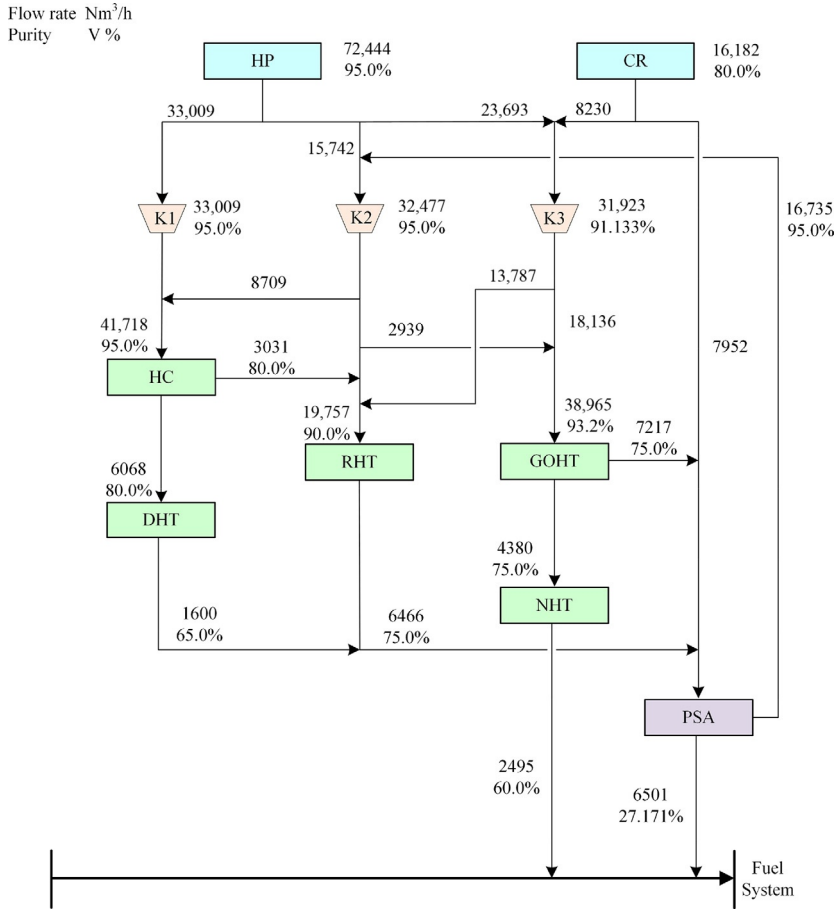

FIG. 13.11 Optimal hydrogen network for Case 2 with the placement of PSA and compressors (Deng et al., 2014).

connections. The decision can be determined according to the plotted Pareto front. With the limitation for the capacity of the purifier, the optimal feed purity for the purifier and number of connections can be determined via minimizing the flow rate of hydrogen utility.

ACKNOWLEDGMENTS

Financial support provided by the National Natural Science Foundation of China (No. 21576287) is gratefully acknowledged. The research is also supported by Science Foundation of China University of Petroleum, Beijing (No. 2462015BJB02 and 2462018BJC003).

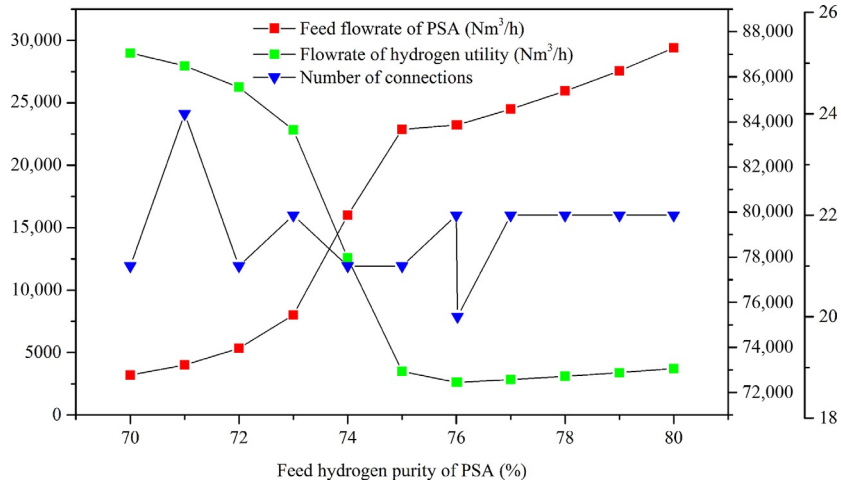

FIG. 13.12 Variation tendency of optimal flow rate of hydrogen utility, feed flow rate of PSA, and total number of connections with the increase of feed hydrogen purity of PSA (Deng et al., 2014).

NOMENCLATURE

Sets and indices

NC	set of components
NF	set of fuel systems
NHU	set of external hydrogen sources or hydrogen utilities
NI	set of compressors
NP	set of hydrogen purifiers
NSK	set of process hydrogen sinks
NSR	set of process hydrogen sources
c	index for component
f	index for fuel system
i	index for compressor
k	index for hydrogen sink
p	index for purifier
s	index for process/internal hydrogen source
u	index for hydrogen utility
ν	index for impurity level

Parameters

$\mathbf{F}_{a,\,b}^{\mathbf{UB}}$	upper bound for flow rate allocated from *a* to *b*
$\mathbf{F}_{a,\,b}^{\mathbf{LB}}$	lower bound for flow rate allocated from *a* to *b*
$\mathbf{FHU}_{u}^{\mathbf{UB}}$	upper bound for the flow rate of *u*th hydrogen utility
$\mathbf{FI}_{i}^{\mathbf{in,\ UB}}$	upper bound for the inlet flow rate of *i*th hydrogen compressor

$\mathbf{FK}_k^{\mathbf{in}}$ inlet flow rate of kth hydrogen sink
$\mathbf{FSR}_s^{\mathbf{UB}}$ upper bound for the flow rate of sth hydrogen source
F_{loss}^{sys} total flowrate loss for direct reuse/recycle system, Nm^3/h
$RR_{p,\,c}$ recovery ratio for cth component in pth purifier
RR hydrogen recovery of purifier
y^{HU} impurity of hydrogen utility, volume fraction
$y_{\mathbf{H}_2}^{arbitrary}$ arbitrary hydrogen purity, volume fraction
$y_{SK_k}^{\mathbf{lim}}$ lower limit of inlet hydrogen purity for hydrogen sinks, volume fraction
$y_{\mathbf{H}_2}^{prod}$ product purity of purifier, volume fraction
$y_{k,\,c}^{\mathbf{in,\,LB}}$ lower bound for inlet concentration for cth component in kth hydrogen sink
$y_{u,\,c}^{\mathbf{out}}$ outlet concentration for cth component in uth hydrogen utility
$y_{s,\,c}^{\mathbf{out}}$ outlet concentration for cth component in sth hydrogen source
$y_{p,\,c}^{\mathbf{prod}}$ concentration for cth component in the product of pth purifier
λ correction coefficient

Variables

$F_{\mathbf{above}}^{\mathbf{pinch}}$ flowrate needed above pinch point, Nm^3/h
F_{net}^{ν} net flowrate in νth impurity level, Nm^3/h
ΔM_{cum}^{ν} cumulative mass load of the νth impurity level, Nm^3/h
F^{feed} feed flowrate of purifier, Nm^3/h
F^{prod} product flowrate of purifier, Nm^3/h
F^{resd} residual flowrate of purifier, Nm^3/h
$y_{\mathbf{H}_2}^{feed}$ feed purity of purifier, volume fraction
$y_{\mathbf{H}_2}^{resd}$ residual purity of purifier, volume fraction
F_{sys}^{resd} residual flowrate of purifier allocated to the direct reuse/recycle system, Nm^3/h
F_{fuel}^{resd} residual flowrate of purifier discharged to the fuel system, Nm^3/h
$Q_{\mathbf{eq}}^{\mathbf{HU}}$ the amount of equivalent energy consumption conservation for the reduction of hydrogen utility, kW

Continuous variables

$F_{a,\,b}$ flow rate allocated from a to b
FF^{in} inlet flow rate for fth fuel system
$FII_{i',\,i}$ flow rate allocated from i'th hydrogen compressor to ith hydrogen compressor
FI_i^{out} outlet flow rate for ith hydrogen compressor
$FIK_{i,\,k}$ flow rate allocated from ith hydrogen compressor to kth hydrogen sink
$FIP_{i,\,p}$ flow rate allocated from ith hydrogen compressor to pth purifier
FI_i^{in} inlet flow rate for ith hydrogen compressor
$FPI_{p,i}^{prod}$ flow rate allocated from the product of pth purifier to ith hydrogen compressor

FP_p^{in} inlet flow rate for pth purifier
FP_p^{prod} flow rate for the product of pth purifier
FP_p^{resd} flow rate for the residual of pth purifier
$FPK_{p,k}^{prod}$ flow rate allocated from the product of pth purifier to kth hydrogen sink
$FPI_{p,i}^{prod}$ flow rate allocated from the product of pth purifier to ith hydrogen compressor
$FPF_{p,f}^{resd}$ flow rate allocated from the residual of pth purifier to fth fuel system
FSR_s flow rate allocated from sth hydrogen source
$FSI_{s,i}$ flow rate allocated from sth hydrogen source to ith hydrogen compressor
$FSK_{s,k}$ flow rate allocated from sth hydrogen source to kth hydrogen sink
$FSP_{s,p}$ flow rate allocated from sth hydrogen source to pth purifier
$FSF_{s,f}$ flow rate allocated from sth hydrogen source to fth fuel system
$FUK_{u,k}$ flow rate allocated from uth hydrogen utility to kth hydrogen sink
$FUI_{u,i}$ flow rate allocated from uth hydrogen utility to ith hydrogen compressor
$y_{i,c}^{in}$ inlet concentration for cth component in ith hydrogen compressor
$y_{i,c}^{out}$ outlet concentration for cth component in ith hydrogen compressor
$y_{p,c}^{in}$ inlet concentration for cth component in pth purifier
$y_{p,c}^{resd}$ concentration for cth component in the residual of pth purifier
$y_{k,c}^{in}$ inlet concentration for cth component in kth hydrogen sink
$y_{f,c}^{in}$ inlet concentration for cth component fth fuel system

Binary variables

$z_{a,b}$ connection variable from a to b
$zIK_{i,k}$ connection variable from ith hydrogen compressor to kth hydrogen sink
$zIP_{i,p}$ connection variable from ith hydrogen compressor to pth purifier
$zII_{i,i'}$ connection variable from i'th hydrogen compressor to ith hydrogen compressor
$zPK_{p,k}^{prod}$ connection variable from the product of pth purifier to kth hydrogen sink
$zPI_{p,i}^{prod}$ connection variable from the product of pth purifier to ith hydrogen compressor
$zPF_{p,f}^{resd}$ connection variable from the residual of pth purifier to fth fuel system
$zSK_{s,k}$ connection variable from sth hydrogen source to kth hydrogen sink
$zSP_{s,p}$ connection variable from sth hydrogen source to pth purifier
$zSI_{s,i}$ connection variable from sth hydrogen source to ith hydrogen compressor
$zSF_{s,f}$ connection variable from sth hydrogen source to fth fuel system

$zUK_{u,k}$ connection variable from uth hydrogen utility to kth hydrogen sink
$zUP_{u,p}$ connection variable from uth hydrogen utility to pth purifier
$zUI_{u,i}$ connection variable from uth hydrogen utility to ith hydrogen compressor

Subscripts/Superscripts

cum cumulative
feed feed of purifier
LB Lower bound
UB Upper bound
prod product of purifier
resd residual of purifier
in inlet
out outlet
lim limiting value
max maximum
min minimum
net net flowrate or load
pinch pinch point
prod product of purifier
resd residual of purifier
SRi ith process hydrogen source
SKk kth process hydrogen sink

Abbreviations

CNHT cracked naphtha hydrotreater
CCR continuous catalytic reforming
GCA gas cascade analysis
GOHT gas oil hydrotreater
IPT Improved Problem Table
HCU hydrocracker unit
LCC Limiting Composite Curve
LP linear programming
MILP mixed integer linear programming
MINLP mixed integer nonlinear programming
MSCC material surplus composite curve
MRPD material surplus composite curve
NLP nonlinear programming
NHT naphtha hydrotreater
NNA nearest neighboring algorithm
PSA pressure swing adsorption
RHS right hand side
RHT residue hydrotreater
TAC total annualized cost
WH waste hydrogen stream

REFERENCES

Agrawal, V., Shenoy, U.V., 2006. Unified conceptual approach to targeting and design of water and hydrogen networks. AICHE J. 52 (3), 1071–1082.

Alves, J.J., Towler, G.P., 2002. Analysis of refinery hydrogen distribution systems. Ind. Eng. Chem. Res. 41 (23), 5759–5769.

Bandyopadhyay, S., 2006. Source composite curve for waste reduction. Chem. Eng. J. 125 (2), 99–110.

Deng, C., Pan, H., et al., 2014. Comparative analysis of different scenarios for the synthesis of refinery hydrogen network. Appl. Therm. Eng. 70 (2), 1162–1179.

Deng, C., Zhou, Y., et al., 2015. Systematic approach for targeting interplant hydrogen networks. Energy 90 (Part 1), 68–88.

El-Halwagi, M.M., Gabriel, F., et al., 2003. Rigorous graphical targeting for resource conservation via material recycle/reuse networks. Ind. Eng. Chem. Res. 42 (19), 4319–4328.

Elkamel, A., Alhajri, I., et al., 2011. Integration of hydrogen management in refinery planning with rigorous process models and product quality specifications. Int. J. Process. Syst. Eng. 1 (3), 302–330.

Foo, D.C.Y., Manan, Z.A., 2006. Setting the minimum utility gas flowrate targets using cascade analysis technique. Ind. Eng. Chem. Res. 45 (17), 5986–5995.

Gary, J.H., Handwerk, G.E., 2001. Petroleum Refining: Technology and Economics. Marcel Dekker, New York.

Hallale, N., Liu, F., 2001. Refinery hydrogen management for clean fuels production. Adv. Environ. Res. 6 (1), 81–98.

Marques, J.P., Matos, H.A., et al., 2017. State-of-the-art review of targeting and design methodologies for hydrogen network synthesis. Int. J. Hydrog. Energy 42 (1), 376–404. https://www.sciencedirect.com/science/article/pii/S0360319916329020.

Prakash, R., Shenoy, U.V., 2005. Targeting and design of water networks for fixed flowrate and fixed contaminant load operations. Chem. Eng. Sci. 60 (1), 255–268.

Rosenthal, R.E., 2010. GAMS-A User's Guide. GAMS Development Corporation, Washington, DC.

Saw, S., Lee, L., et al., 2011. An extended graphical targeting technique for direct reuse/recycle in concentration and property-based resource conservation networks. Clean Techn. Environ. Policy 13 (2), 347–357.